

Lengths of CFRP Laminates at Zone of Hogging Moment for T-Section Continuous RC Beams (Part I)

Mohammad Mohie Eldin¹, Ahmed M. Tarabia² and Rahma Faraj³

¹Department of Civil Engineering, Faculty of Engineering, Beni-Suef University, Egypt

²Department of Structural Engineering, Faculty of Engineering, Alexandria University, Egypt

³Department of Civil Engineering, Faculty of Engineering, Sirte University, Libya

mohammad_mohie_eldin@yahoo.com

Abstract: Carbon fiber reinforced polymer (CFRP) laminates were proved as very effective method for either repairing or strengthening of used structures. However, the literature has no enough information about the behavior of RC continuous (two-span) T-section beams strengthened with CFRP laminates, especially in hogging moment zone. This paper examines the effect of CFRP laminates lengths, used for strengthening of the hogging moment zone, upon the behavior of such beams, to determine the optimum strengthening length. 3-D theoretical models using the Finite Element (FE) Package ANSYS are used. Very good agreement was found between both proposed FE models and previous experimental research used for the verification of the FE model. Finally, redistribution of moments, energy dissipation and ductility of such beams are examined. It can be concluded that changing the strengthening CFRP length in the hogging moment zone is very effective upon the overall behavior of T-section continuous beams and their reinforcement bars.

[Mohammad Mohie Eldin, Ahmed M. Tarabia and Rahma Faraj. **Lengths of CFRP Laminates at Zone of Hogging Moment for T-Section Continuous RC Beams (Part I)**. *J Am Sci* 2016;12(12):62-70]. ISSN 1545-1003 (print); ISSN 2375-7264 (online). <http://www.jofamericanscience.org>. 8. doi:[10.7537/marsjas121216.08](https://doi.org/10.7537/marsjas121216.08).

Keywords: CFRP, continuous, beam, RC, strengthen, hogging, T-section, length, ANSYS.

Introduction

Only little literature are available considering the behavior of two-span continuous beams with rectangular sections strengthened using CFRP laminates. Experimentally, an external strengthening using CFRP laminates was found to increase the load capacity of such beams. Also, moment redistribution in such beams is possible if the longitudinal and transverse reinforcement configuration is chosen properly [1]. Increasing the number of CFRP layers, not beyond its optimum value, increases both flexure and shear strength and capacity. However, it decreases ductility, moment redistribution, and ultimate strain on CFRP laminates [2, 3 and 4]. Extending the CFRP length to cover the entire hogging or sagging zones did not prevent peeling failure of the CFRP laminates [3]. It was shown that the debonding mechanisms are governed by shear forces and moment redistribution occurring in multi-span beams [5]. Adding to thickness of CFRP laminates and strengthening of both hogging and sagging regions, end anchorage techniques are effective upon the response of reinforced high strength concrete (RHSC) continuous beams [2].

It was shown that externally strengthened RC beams with bonded CFRP laminates have significant increases in their ultimate loads [6]. CFRP strengthened cross-sections restrict the rotation of plastic hinges at their locations, and allow additional plastic hinges formation in unstrengthened cross-sections [5]. On the other side, T-section beams are

very important since it takes into account the interaction between both beams and slabs. However, very rare research is available about T-section simple or continuous beams strengthened using CFRP laminates. M. M. Rahman *et al.* [7] presented an effective technique of applying CFRP laminate for strengthening the hogging zone of continuous T beam considering column constrains. The purpose of this paper is to investigate the effect of CFRP laminates lengths upon strengthening of T-section continuous (two spans) beams in the hogging moment zone; above and around the intermediate support.

Verification of FE mode

FE model used in this paper was verified through the beam (B2) used in the experimental program made by Saleh and Barem (2013) as shown in Figures (1) and (2).

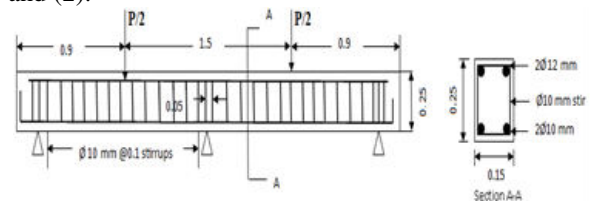


Figure (1): Details of Beam (B2).

They were at top face of beam at the negative zone and bottom face of beam at the positive zones. External anchorages used in this study were made from CFRP U-shape at the end of longitudinal CFRP

laminates. Thickness of used CFRP laminates is 0.113 mm.

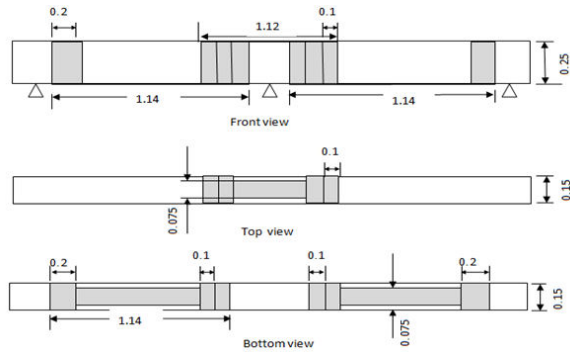


Figure (2): CFRP Locations and Anchors (in meters)

1.1 Finite Element Modeling

1.1.1 Element Types

Five types of finite elements; SOLID65, LINK180, SHELL181, CONTA173, and TARGET170 are used for 3-D modeling of the tested beams, as follows:

- **SOLID65** is defined by eight nodes having three degrees of freedom at each node: translations in the nodal x, y, and z directions. The solid is capable of cracking in tension and crushing in compression. It is used for the modeling of concrete elements.
- **LINK180** is a uniaxial tension-compression element with three degrees of freedom at each node: translations in the nodal x, y, and z directions. It is used for the modeling of steel reinforcement bars and stirrups.
- **SHELL181** is a 4-node element with six degrees of freedom at each node: translations in the x, y, and z directions, and rotations about the x, y, and z-axes. As it may be used for layered applications for modeling laminated composite, it is used for the modeling of CFRP laminates.
- **CONTA173** is a 3-D contact element that is used to represent contact and sliding between “target” surface and a deformable contact surface.
- **TARGE170** is a 3-D target element that is used to represent 3-D “target” surfaces for the associated contact elements (CONTA173).

Target surface is the surface of concrete beam and the deformable contact surface is that of CFRP laminates. Both contact and target elements form what is called “Contact Pair”.

Different types of contact pairs are available from “standard” to “full bond”. The used type is “initially bonded” which allows, with loading increasing, both sliding and gap between the two surfaces of the contact pair.

- Elements have plasticity, large deflection, and large strain capabilities.

1.1.2 Material properties

Concrete: Stress-strain curve of concrete was modeled using the equations of Thorenfeldt *et al.* (1987). These equations are mainly functions in the value of the compression strength of concrete (F_c). Figure (3) shows a typical RC stress-strain curve. Additional concrete material data related to SOLID65 element have to be input; shear transfer coefficients and tensile stresses. Shear transfer coefficients range from 0.0 (representing a smooth crack or complete loss of shear transfer) to 1.0 (representing a rough crack or no loss of shear transfer). This specification may be made for both open and closed crack. Open-crack and close-crack shear coefficients are taken as 0.1 and 0.9, respectively. Ultimate tensile strength F_t is taken as 10-15% of the compression strength. When the element is cracked or crushed, a small amount of stiffness is added to the element for numerical stability. However, crushing capability was turned off to allow convergence of the models. Also, secant modulus of elasticity is used in the FE modeling instead of the initial one. Finally, Poisson’s ratio is taken as 0.2.

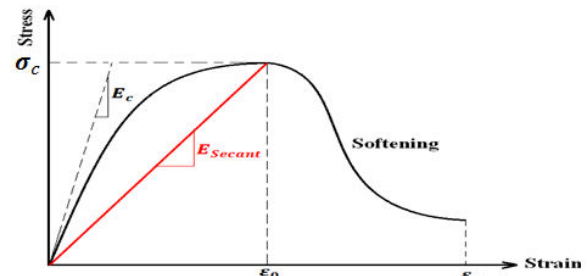


Figure (3): Typical RC Stress-Strain Curve.

Steel: Bilinear isotropic hardening material is used to represent the stress-strain curve of steel bars. Required data are Modulus of elasticity ($E_s = 200,000 \text{ MPa}$), Poisson’s ratio ($\nu_s = 0.3$), and yield stress (σ_y).

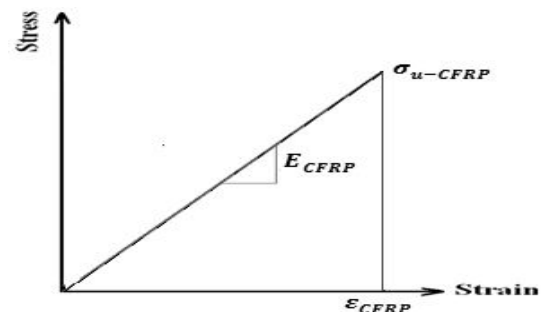


Figure (4): Typical CFRP Stress-Strain Curve.

CFRP: Multilinear isotropic hardening material is used to represent the stress-strain curve of CFRP laminates shown in Figure (4) The behavior is linear till its maximum stress and then dropped to zero stress at maximum strain.

1.1.3 Meshing

Meshing analysis was done to obtain the acceptable size of solid elements that lead to accurate results in a minimum solution time. As a result, element size of: ($x \times y \times z = 50 \times 50 \times 50$ mm) was chosen.

1.1.4 Boundary conditions

The outer two supports are modeled as roller supports to only allow the movement in the direction of the beam axe (direction Z), while the mid-support is pinned support to prevent it from movement in any direction. According to symmetry, only one quarter of the beam is modeled with the application of boundary conditions at the two planes of symmetry.

1.1.5 Yield Criterion

Von Mises yield criterion is used to predict the onset of the yielding, whereas the behavior upon further yielding is predicted by the ‘flow rule’ and ‘hardening law’.

1.2 Results

Figure (6) shows load vs. Mid-Span-deflection of beam (B2) due both experimental and FE results. Very good agreement is achieved that insure using ANSYS as a modeling tool for continuous RC beams strengthened by CFRP laminates.

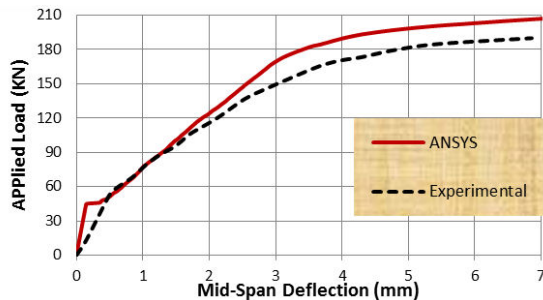


Figure (6): Results of Beam (B2).

2. Parametric Study

2.1 Dimensions of Modeled Beams

A continuous beam of two spans and T-cross-section is used for the parametric study. The beam is 6000 mm span length, 300 mm web width, 700 mm beam depth, 140 mm flange depth, and 1140mm flange width, as shown in Figure (7). Each span is loaded by two concentrated loads (P) at third and two thirds of the span length. Such beam is subjected to sagging moment along spans and hogging moment at the interior support, as shown in Figure (8). It is obvious that the length of the hogging moment zone (HMZ) equals $(3/4 L_1)$ or 1500 mm for each of the two spans. The beam was designed using the Egyptian Code of Practice ECP-203 (2007). CFRP laminate has width equals to the web width (300 mm) and its length equals $(2L_2)$; (L_2) above each span, as shown in Figure (7).

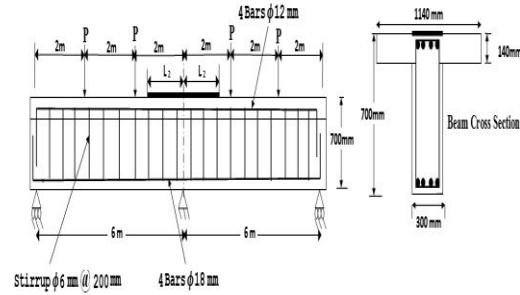


Figure (7): Dimensions and Reinforcement.

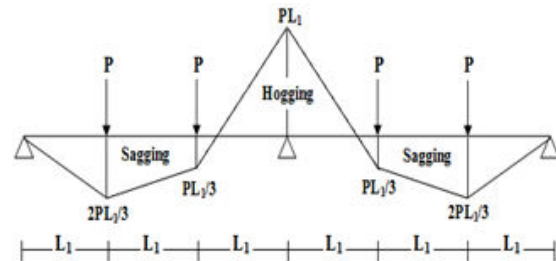


Figure (8): Bending Moment Diagram.

The Egyptian Code ECP-208 (2005) was used to design the suitable thickness of the CFRP laminates which was approximated as 0.9 mm. However, the designed upper reinforcement at the hogging moment zone was reduced by 75% from (4-bars ϕ 24mm) to (4-bars ϕ 12mm) to allow good investigation of the effect of CFRP strengthening laminates in this zone. The following table (1) shows mechanical properties of the used materials; concrete, steel, and CFRP.

Table (1): Mechanical Properties of Materials.

Concrete (MPa)			Steel	Bras	CFRP Laminates (MPa)	
σ_c	σ_t	E_c	σ_y	E_s	σ_{u-CFRP}	E_{CFRP}
30	3	26000	400	200000	3050	165000

2.2 Investigated CFRP Lengths, Loading Stages and FE Modeling

Adding to the control beam, five lengths of CFRP laminates are used to investigate the effect of CFRP strengthening length upon the behavior of the beams. These lengths are ($0.267L_{HMZ} = 400$) ($0.4L_{HMZ} = 600$), ($0.6L_{HMZ} = 900$), ($0.80L_{HMZ} = 1200$), and ($L_{HMZ} = 1500$) per each of the two spans measured from the mid-support. For each of the beams, five stages of loading were studied to analyze the behavior. These stages are:

- i. At first crack.
- ii. Between first crack and steel yield.
- iii. At steel yield.
- iv. Between steel yield and failure.
- v. At failure.

Beams were modeled in the same procedure of FE modeling mentioned in Section 2.1.

2.3 Results and Discussions

2.3.1 Load - Deflection Relation

Figure (9) shows the relation between the applied load at each span (2P) and the maximum deflection (at the point of maximum moment). The effect of strengthening appears just after first-cracking of the beams. This means that the effect of both CFRP laminates and steel bars is synchronous. Also, it is obvious that increasing CFRP length increases both capacity(maximum moment) and ductility (related to maximum deflection) of the beam. Figure (10) shows the relation between strength (maximum applied load) of the beams via the ratio between CFRP length (L_2) and the length of hogging moment zone (HMZ). It is approximately linear till a certain length and then it is constant. This means that there is an optimum length ($L_2 = 0.8L_{HMZ}$) for strengthening with CFRP laminates, if the capacity is the goal of the strengthening.

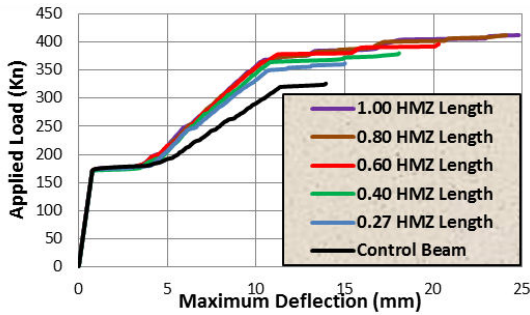


Figure (9): Load – Deflection Curve.

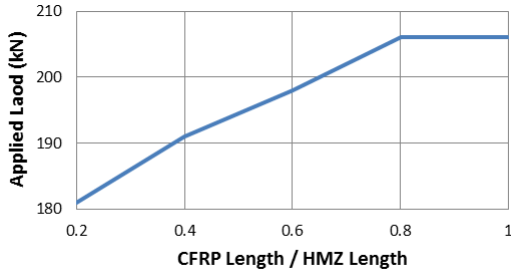


Figure (10): Load Versus (L_2/L_{HMZ}) Ratio.

2.3.2 Stresses of CFRP Laminates at Different Stages of Loadings

Figures (11)-(15) show stresses distribution of CFRP laminates along their lengths, measured from the mid-support, at the five stages of loading. Due to the elastic behavior of CFRP, strains distributions are identical to that of the stresses.

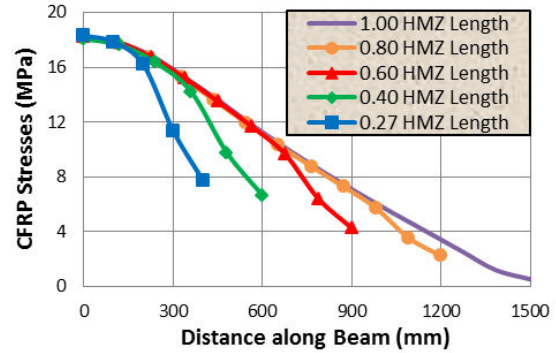


Figure (11): CFRP Stresses at First Stage.

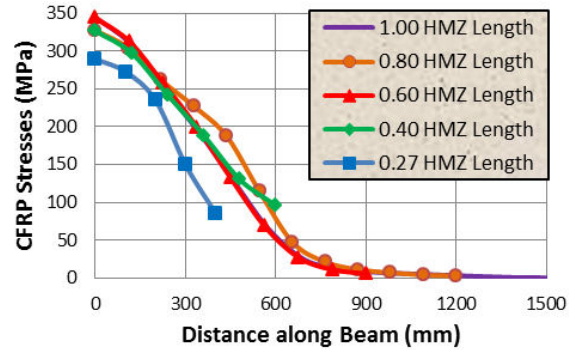


Figure (12): CFRP Stresses at Second Stage.

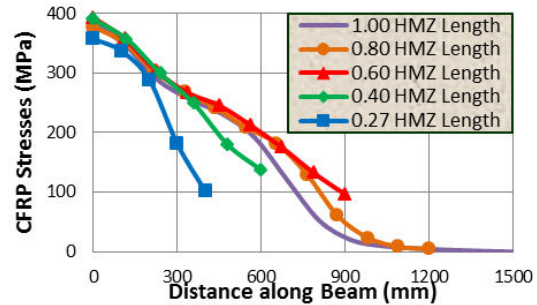


Figure (13): CFRP Stresses at Third Stage.

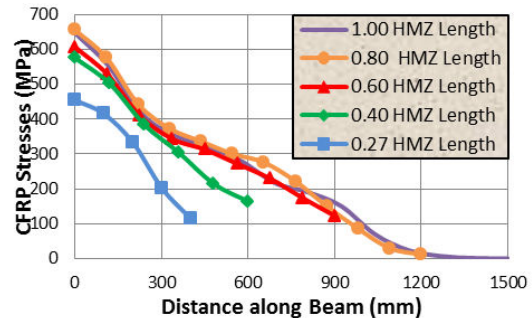


Figure (14): CFRP Stresses at Fourth Stage.

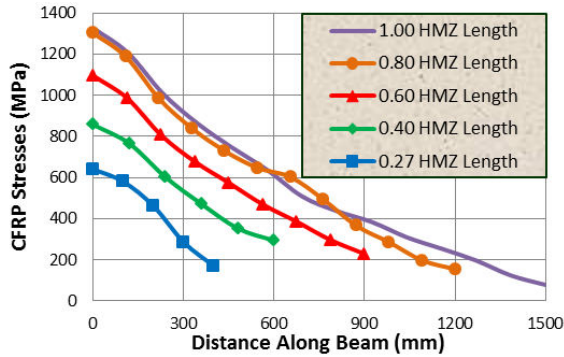


Figure (15): CFRP Stresses at Fifth Stage.

According to figures, the following may be concluded:

1. Maximum stresses (strains) lie at the mid-support and decrease gradually till the ends of the laminates.
2. Effect of strengthening with CFRP laminates begins just after the first crack of the concrete. However, the effect of CFRP length is becoming increasingly apparent and influential after yielding of upper steel bars.
3. At the same distance from the mid-support, CFRP laminates with greater lengths bear greater stresses.
4. At their ends, CFRP laminates with greater lengths have less stresses.
5. This means that increasing the length of CFRP laminate maximize its benefits and decrease concentration of stresses at its end.

6. According to Figures (12)-(15), stresses at the beginnings of CFRP laminates for both lengths 1200 and 1500 mm are very close and can be considered as equal. These stresses are the biggest comparing with other CFRP lengths.

7. According to Figures (12)-(14), stresses at the ends of CFRP laminates for both lengths 1200 and 1500 mm are approximately the same and equal or close to zero, while these stresses are of considerable values for other lengths.

8. As a conclusion, the optimum length considering the distribution of stresses/strains along both CFRP length and length of HMZ is ($L_2 = 0.8L_{HMZ}$).

2.3.3 Stresses/Strains for Each individual CFRP Length

It was found that the behavior in all the stages of loading is the same for all the lengths. So, only the results of lengths; 600, 1200 and 1500mm (0.4, 0.8 and 1.0 HMZ Length), will be shown in Figures (16) and (17). Again and due to elastic behavior of CFRP, strains distributions are identical to that of the stresses. According to results, the following may be concluded:

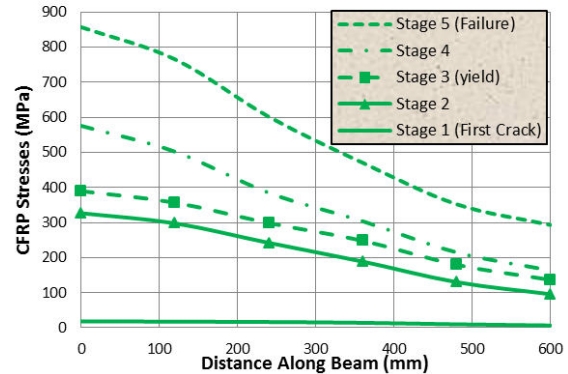


Figure (16): Stresses along CFRP length ($L_2 = 0.4 L_{HMZ}$)

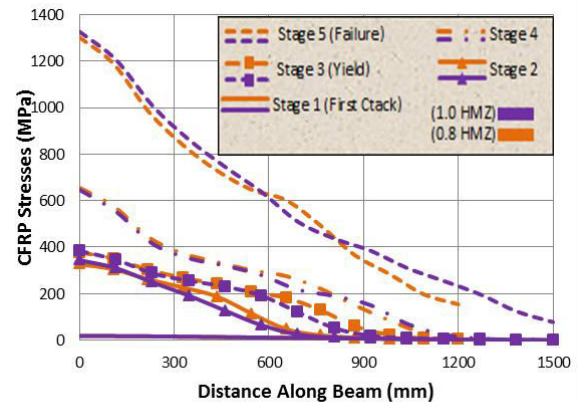


Figure (17): Stresses along CFRP ($L_2 = 0.8$ and $1.0 L_{HMZ}$)

1. It confirms that no effect for the CFRP laminates before first cracking of concrete.

2. Before steel yielding, CFRP stresses are less than yield stress of steel. This means less utilizing of CFRP.

3. After steel yielding, increasing CFRP lengths increases their stresses beyond yield stress of steel, at mid-support, which means more utilizing of strengthening till failure. However, this increasing will approximately vanish at a certain CFRP length ($L_2 = 0.8L_{HMZ}$).

4. Maximum contribution of the CFRP laminates in strengthening lies after yielding of steel.

5. At yielding of steel for the 1500mm-length CFRP laminate, the length of zero-stresses-part is about 500 mm which means that about 33% of the length is useless at this stage. This percentage decreases to about 16.5% in the stage (4).

6. However, at yielding of steel for the 1200mm-length CFRP laminate, the length of zero-stress-part is about 150 mm which means that only

12.5% of the length is useless. However, this percentage decreases to about zero in the stage (4).

7. This insures that CFRP length of ($L_2 = 0.8L_{HMZ}$) is the optimum length.

2.3.4 Stresses and Strains in Upper Steel Bars at Different Stages of Loadings

Figures (18)-(20) show stresses in the upper steel bars along their lengths until steel yielding. Both stresses and strains are relative due elastic behavior of steel in these stages of loading. Figures (21)-(24) show stresses and strains for the last two stages of loading; after steel yield and till failure. According to the results, the following may be concluded:

1. Stresses are not affected by the presence of CFRP laminates, whatever their lengths, until the first crack of concrete.

2. Stresses (strains) of steel bars are of maximum value at mid-support and decrease gradually as a general along their length.

3. For strengthening length of 400mm, stresses and strains of upper steel bars increase suddenly and sometimes dramatically at the end of CFRP Laminates. This happens to some extent with 600mm CFRP length.

4. Stresses/strains for CFRP lengths 1200 and 1500 mm are very close, especially after steel yielding.

5. At failure, increasing the lengths of CFRP laminates increases the yielded length of upper steel bars.

6. Increasing the lengths of CFRP laminates improves strains distribution and, to some extent, stresses distribution of upper steel bars. So, it improves the utilizing of upper steel bars.

7. According to the behavior of upper steel bars the optimum CFRP length is ($L_2 = 0.8L_{HMZ}$), while the minimum length has to be more than $0.4L_{HMZ}$.

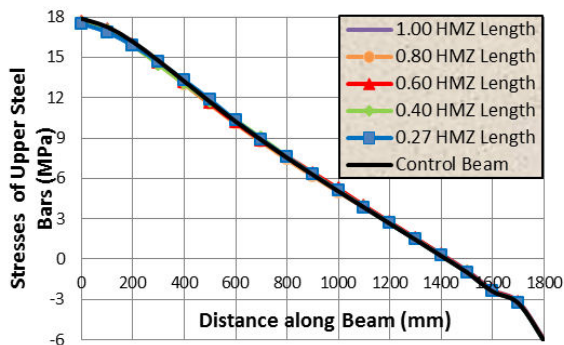


Figure (18): Stresses in Upper Steel Bars at First Crack.

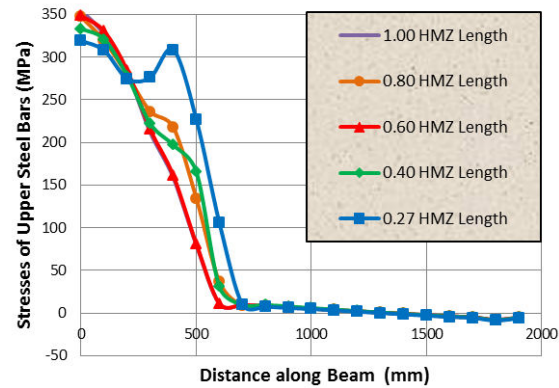


Figure (19): Stresses in Upper Steel Bars at Second Stage.

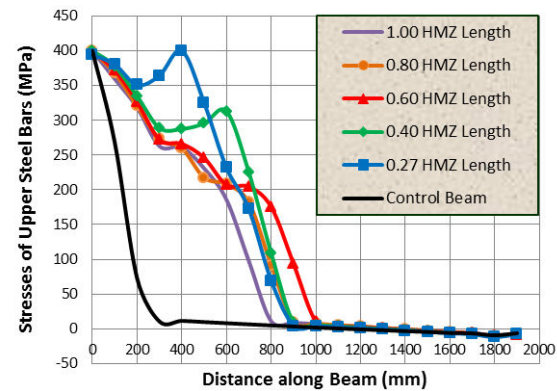


Figure (20): Stresses in Upper Steel Bars at Steel Yield.

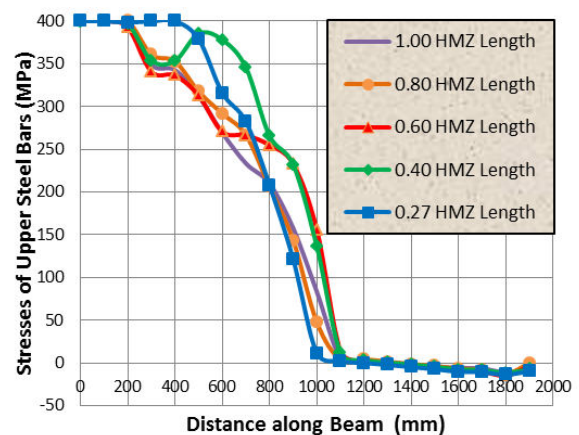


Figure (21): Stresses in Upper Steel Bars at Fourth Stage.

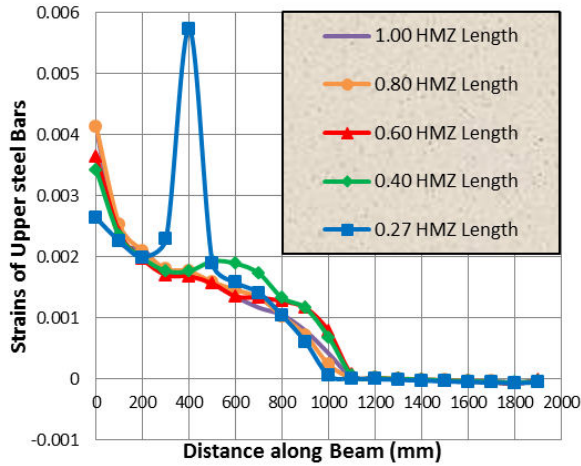


Figure (22): Strains in Upper Steel Bars at Fourth Stage.

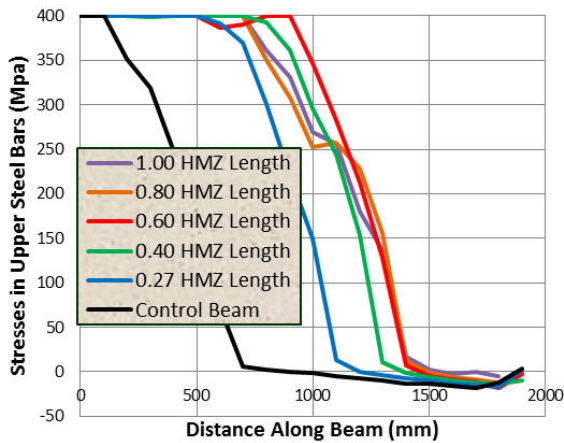


Figure (23): Stresses in Upper Steel Bars at Failure.

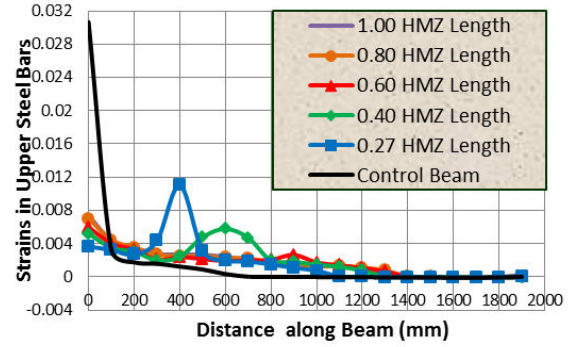


Figure (24): Strains in Upper Steel Bars at Failure.

2.3.5 Moment Redistribution

In this section, redistribution of moments between both sagging and hogging moments is examined. This redistribution allows good utilizing of the beam capacity.

Moment redistribution factor (β) is defined as: $\beta = \left(\frac{M_{FE} - M_E}{M_E} \right) \times 100\%$ (1)

Where M_{FE} is the bending moment calculated from FE results at failure (using both failure loads and their corresponding reactions), and M_E is the failure bending moment calculated elastically due to applied loading at failure. Figure (25) shows diagrams for the control beam (CB) and the strengthened beams BS1, BS2, BS3, BS4 and BS5 with CFRP lengths 400, 600, 900, 1200 and 1500 mm, respectively, for both M_{FE} and M_E . Only one span is drawn due symmetry. Table (2) contains values of the redistribution ratio (β) for the different beams which is negative at mid-support and positive at span. This means decreasing of the hogging moments (at mid-support) and increasing of sagging moments (at span).

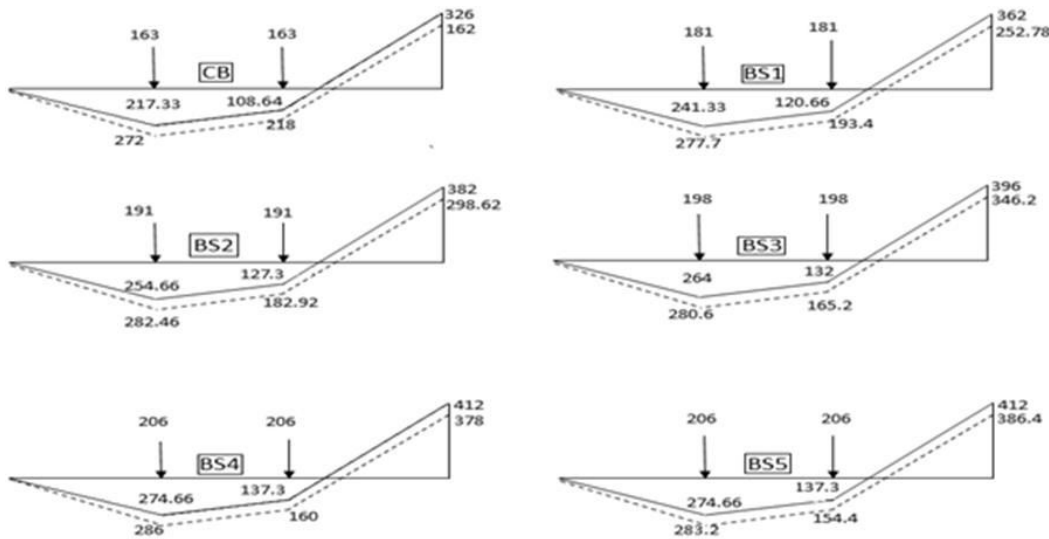


Figure (25): Redistribution of Moments: (M_E —) and (M_{FE} - - -) Moments Diagrams.

Table (2): Values of Moment Redistribution Factor (β).

Beam	P_u (KN)	Reactions (KN)		Mid-Support			Span		
		Mid-Support	End Support	M_{FE} (KN.m)	M_E (KN.m)	β (%)	M_{FE} (KN.m)	M_E (KN.m)	β (%)
CB	326	189.91	136.09	162.00	326	-50.31	272.18	217.00	25.43
BS1	362	223.13	138.87	252.78	362	-30.17	277.70	241.33	15.07
BS2	382	240.77	141.23	298.62	382	-21.83	282.48	254.66	10.92
BS3	396	253.70	142.30	346.20	386	-10.31	280.60	264.00	6.29
BS4	412	268.98	143.02	378.00	412	-8.25	286.00	274.66	4.13
BS5	412	270.33	141.67	386.40	412	-6.21	283.20	274.66	3.11

According to Table (2), it can be seen that increasing the length of CFRP laminates decreases the absolute value of the moment redistribution factor (β). This means that a plastic hinge will be made up after decreasing the hogging moment according to redistribution. However, this plastic hinge will not cause failure, since and due to continuity of moment redistribution, sagging moment will increase till failure. This means that increasing the CFRP

laminates lengths improves the utility of the moment capacity of the beam either positive or negative.

2.3.6 Energy Dissipation and Ductility

Figure (26) shows the definition of the energy dissipation by the continuous beam at the yielding of upper steel (E_y) and at failure (E_u). Ductility index (μ_D) and energy dissipation index (μ_E) are defined as:

$$\mu_D = \frac{\Delta_u}{\Delta_y} \quad (2)$$

$$\mu_E = \frac{E_u}{E_y} \quad (3)$$

Table (3): Values of ductility index μ_D and energy dissipation index μ_E

Beam	(Δ_y) m	(Δ_u) mm	$\mu_D = \frac{\Delta_u}{\Delta_y}$	Increase over CB (%)	(E_y) KN.mm	(E_u) KN.mm	$\mu_E = \frac{E_u}{E_y}$	Increase over CB (%)
CB	11.2	13.8	1.232	-----	2408.756	3243.356	1.346	-----
BS1	10.8	14.9	1.380	11.970	2434.412	3894.012	1.600	18.796
BS2	10.8	18	1.667	35.266	2468.156	5117.756	2.073	53.994
BS3	10.8	20.1	1.861	51.047	2563.796	6125.696	2.389	77.448
BS4	10.1	23.5	2.327	88.836	2314.316	7486.716	3.235	140.252
BS5	10.1	24.8	2.455	99.283	2314.316	7988.516	3.452	156.355

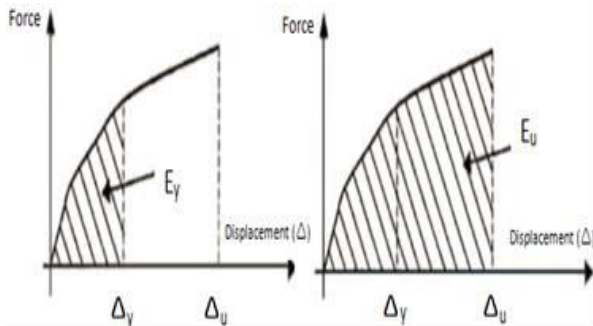


Figure (26): Definition of Ductility and Moment Capacity.

Where Δ_y and Δ_u are deflections at yielding of steel and at failure, respectively.

Table (3) shows the values of both ductility and energy dissipation indexes for the different beams, and comparing with the control one.

Increasing the length of CFRP laminate increases both ductility index and energy dissipation index, which means a very good utilizing of the beam after yielding of upper steel bars. Both capacity (strength) and ductility of the strengthened beam increase very much with increasing of the CFRP laminate length.

Conclusions

- Effect of strengthening with CFRP laminates begins just after the first crack of the concrete.
- Stresses (strains) of CFRP laminates are of maximum value at mid-support and decrease gradually along their length.
- Maximum contribution of the CFRP laminates in strengthening lies after yielding of steel.

iv. Increasing the length of CFRP laminate maximize its benefits and decrease concentration of stresses at its end.

v. Stresses (strains) of steel bars are of maximum value at mid-support and decrease gradually as a general along their length.

vi. Increasing the lengths of CFRP laminates improves strains distribution and, to some extent, stresses distribution of upper steel bars. So, it improves the utilizing of upper steel bars.

vii. Increasing the length of CFRP laminates improves, very much, the redistribution of moments between sagging and hogging moments. This means much more utilizing of the moment capacity of the beam either positive or negative.

viii. Increasing the lengths of CFRP laminates increase both ductility and energy dissipation of the beam (its moment capacity or strength).

ix. The optimum length of CFRP laminate, neglecting the effect of the area of the upper reinforcement, is ($L_2 = 0.8L_{HMZ}$), while the minimum length has to be more than $0.4L_{HMZ}$.

x. It is believed that the optimum length of CFRP laminate should change with the change of the upper reinforcement. As a result, complementary research is under performing to relate between both the optimum length of CFR laminate and the reinforcement.

Reference

1. M. El-Mogy, A. El-Ragaby, and E. El-Salakawy, "Experimental testing and finite element modeling on continuous concrete beams reinforced with fibre reinforced polymer bars and stirrups", *Canadian Journal of Civil Engineering*, Vol. 40, No. 11, pp. 1091–1102, November 2013.
2. A. A. Maghsoudi, H. A. Bengar, "Moment redistribution and ductility of RHSC continuous beams strengthened with CFRP", *Turkish Journal of Engineering and Environmental Sciences*, <http://journals.tubitak.gov.tr/engineering/issues/muh-09-33-1/muh-33-1-5-0901-6.pdf>, Vol. 33, pp. 45-59, 2009.
3. S. A. El-Refaie, A. F. Ashour, and S. W. Garrity, "Sagging and Hogging Strengthening of Continuous Reinforced Concrete Beams Using Carbon Fiber-Reinforced Polymer Laminates", *ACI Structural Journal*, V. 100, No. 4, pp. 446-453, July-August 2003.
4. W. M. Iesa, M. B. S. Alferjani, N. Ali, and A. A. Abdul Samad, "Study on Shear Strengthening of RC Continuous Beams with Different CFRP Wrapping Schemes", *International Journal of Integrated Engineering (Issue on Civil and Environmental Engineering)*, <http://penerbit.uthm.edu.my/ojs/index.php/ijie/article/view/207>, Vol. 2, No. 2, pp. 35-43, 2010.
5. L. Taerwe, L. Vasseur, and S. Matthyss, "External strengthening of continuous beams with CFRP", *Concrete Repair, Rehabilitation and Retrofitting II*, London, ISBN 978-0-415-46850-3, pp. 43-53, 2009.
6. A. R. Saleh, and A. A. H. Barem, "Experimental and Theoretical Analysis for Behavior of R.C. Continuous Beams Strengthened by CFRP Laminates", *Journal of Babylon University (Iraq), Engineering Sciences*, Vol. 21, No. 5, pp. 1555-1567, 2013.
7. M. M. Rahman, and M. W. Rahman, "Simplified method of strengthening RC continuous T beam in the hogging zone using carbon fiber reinforced polymer laminate - A numerical investigation", *Journal of Civil Engineering Construction Technology*, <http://www.academicjournals.org/JECET>, ISSN 1991-637X, Vol. 4, No. 6, pp. 174-183, June 2013.
8. ANSYS, "ANSYS Help", Release 15.0, 2013.
9. Thorenfeldt E., A. Tomaszewicz, and J. Jensen, "Mechanical Properties of High Strength Concrete and Application to Design," *Proceedings of the Symposium: Utilization of High-Strength Concrete*, Stavanger, Norway, Tapir, Trondheim, pp. 149–159, June 1987.
10. "ECP-203: Egyptian Code of Practice for the Design and Implementation of Reinforced Concrete Structures", *Housing and Building Research Center (HBRC), Cairo, Egypt*, 2007.
11. "ECP-208: Egyptian Code for the Design Principals and Implementation Requirements of Using CFRP in Fields of Construction, Housing and Building Research Center (HBRC), Cairo, Egypt, 2005.
12. Sakr M. A., T. M. Khalifa, and W. N. Mansour, "External Strengthening of RC Continuous Beams Using FRP Plates: Finite Element Model", *Proc. of the Second Intl. Conf. on Advances in Civil, Structural and Mechanical Engineering- CSM 2014*, ISBN: 978-1-63248-054-5, pp. 168-174, 2014.